J Prev Alz Dis 2024;2(11):435-444
Published online January 8, 2024, http://dx.doi.org/10.14283/jpad.2023.134

Original Research

Personalized Computational Causal Modeling of the Alzheimer Disease Biomarker Cascade

*J.R. Petrella[1], J. Jiang[1], K. Sreeram[1], S. Dalziel[1], P.M. Doraiswamy[2], W. Hao[3], for the Alzheimer's Disease Neuroimaging Initiative***

1. Department of Radiology, Duke University School of Medicine, DUMC - Box 3808 , 27710-3808, NC, USA; 2. Departments of Psychiatry and Medicine, Duke University School of Medicine; Duke Institute for Brain Sciences, DUMC - Box 3808 , 27710-3808, NC, USA; 3. Department of Mathematics, Pennsylvania State University, McAllister Bldg 208, 16802, PA, USA

Corresponding Author: Jeffrey R. Petrella, Department of Radiology, Duke University School of Medicine, DUMC - Box 3808 , 27710-3808, NC, USA jeffrey.petrella@duke.edu

Abstract

BACKGROUND: Mathematical models of complex diseases, such as Alzheimer's disease, have the potential to play a significant role in personalized medicine. Specifically, models can be personalized by fitting parameters with individual data for the purpose of discovering primary underlying disease drivers, predicting natural history, and assessing the effects of theoretical interventions. Previous work in causal/mechanistic modeling of Alzheimer's Disease progression has modeled the disease at the cellular level and on a short time scale, such as minutes to hours. No previous studies have addressed mechanistic modeling on a personalized level using clinically validated biomarkers in individual subjects.

OBJECTIVES: This study aimed to investigate the feasibility of personalizing a causal model of Alzheimer's Disease progression using longitudinal biomarker data.

DESIGN/SETTING/PARTICIPANTS/MEASUREMENTS: We chose the Alzheimer Disease Biomarker Cascade model, a widely-referenced hypothetical model of Alzheimer's Disease based on the amyloid cascade hypothesis, which we had previously implemented mathematically as a mechanistic model. We used available longitudinal demographic and serial biomarker data in over 800 subjects across the cognitive spectrum from the Alzheimer's Disease Neuroimaging Initiative. The data included participants that were cognitively normal, had mild cognitive impairment, or were diagnosed with dementia (probable Alzheimer's Disease). The model consisted of a sparse system of differential equations involving four measurable biomarkers based on cerebrospinal fluid proteins, imaging, and cognitive testing data.

RESULTS: Personalization of the Alzheimer Disease Biomarker Cascade model with individual serial biomarker data yielded fourteen personalized parameters in each subject reflecting physiologically meaningful characteristics. These included growth rates, latency values, and carrying capacities of the various biomarkers, most of which demonstrated significant differences across clinical diagnostic groups. The model fits to training data across the entire cohort had a root mean squared error (RMSE) of 0.09 (SD 0.081) on a variable scale between zero and one, and were robust, with over 90% of subjects showing an RMSE of < 0.2. Similarly, in a subset of subjects with data on all four biomarkers in at least one test set, performance was high on the test sets, with a mean RMSE of 0.15 (SD 0.117), with 80% of subjects demonstrating an RMSE < 0.2 in the estimation of future biomarker points. Cluster analysis of parameters revealed two distinct endophenotypic groups, with distinct biomarker profiles and disease trajectories.

CONCLUSION: Results support the feasibility of personalizing mechanistic models based on individual biomarker trajectories and suggest that this approach may be useful for reclassifying subjects on the Alzheimer's clinical spectrum. This computational modeling approach is not limited to the Alzheimer Disease Biomarker Cascade hypothesis, and can be applied to any mechanistic hypothesis of disease progression in the Alzheimer's field that can be monitored with biomarkers. Thus, it offers a computational platform to compare and validate various disease hypotheses, personalize individual biomarker trajectories and predict individual response to theoretical prevention and therapeutic intervention strategies.

Key words: Mathematical modeling, dementia, Alzheimer's disease, disease.

Introduction

Alzheimer's disease (AD) progression, from presymptomatic to late-stage disease, can be tracked in individual patients through several validated biomarkers of amyloid, tau and neurodegenerative pathology. Most studies of AD biomarkers have been correlational, using statistical models to find associations among individual biomarkers or between individual biomarkers and other disease risk factors such as genetics or cardiovascular disease, for example. Such models are limited, however, in their ability to treat biomarkers interdependently or make causal inferences about disease mechanisms and therapeutic responses. Causal or explanatory disease models, on the other hand, are a class of models that relate experimental data to a biological process underlying the phenomenon under investigation (1). Such models integrate prior knowledge, help elucidate underlying mechanisms, and allow predictions about the response to therapy. Theoretically, such models can be personalized by fitting parameters with individual data with the purpose of discovering primary underlying

Received July 27, 2023
Accepted for publication September 29, 2023

disease drivers, predicting natural history, and ultimately, assessing the effects of theoretical interventions on biomarkers and clinical outcomes. The purpose of this study was to explore the feasibility of personalizing a time-dependent causal model of AD progression with longitudinal biomarker data. As a proof of concept, we chose the AD Biomarker Cascade (ADBC) model, a widely referenced hypothetical model of AD, based on the amyloid cascade hypothesis. The model integrates four key biomarkers of AD progression: pathologic hallmark biomarkers beta-amyloid and tau, neuronal loss biomarkers, and cognitive impairment biomarkers (2, 3). It has recently been formulated mathematically and implemented computationally to generate intuitively sound predictions of biomarker trajectories over time (4). In this study, we build upon these results by parameterizing and testing personalized models in over 800 subjects with serial biomarker data from the Alzheimer Disease Neuroimaging Initiative (ADNI), a multicenter, prospective, naturalistic study that includes genetic, clinical, body fluid, and imaging data (https://adni.loni.usc.edu).

Methods

The ADBC Model

The ADBC model has been described in detail by Jack et al. (2, 3), and its mathematical formulation by Petrella et al. (4). Briefly, the ADBC model postulates that AD is caused by a cascade of pathophysiological changes, characterized by time-dependent alterations in four key biomarkers of AD progression described above (Figure 1). The cascade is initiated by over-production, and/or under- clearance of amyloid protein from the brain. The buildup of the amyloid pool leads to the initiation of a tau protein cascade, and subsequently, a neurodegeneration cascade, resulting in progressive cognitive decline. Other, suspected non-AD-related pathologies (SNAP), such as cerebrovascular disease, age- related changes, and non-AD tauopathies, may also contribute to the neurodegenerative cascade and, in turn, to cognitive decline. The onset and rate of cognitive decline are modulated by genetic risk, as well as factors that influence cognitive reserve capacities, such as education or other contributors to cognitive resilience. Potential therapies, such as anti-amyloid treatments, which increase the clearance of the amyloid pool, have previously been added to the model to simulate optimize therapeutic effects on biomarkers while minimizing side effects (5).

The mathematical formulation of the ADBC model consists of an interdependent system of ordinary differential equations characterizing the rates of change and initial conditions of each of the biomarker pools,

$$\begin{cases} \frac{dA_\beta}{dt} = \lambda_{A_\beta} A_\beta (K_{A_\beta} - A_\beta) \\ \frac{d\tau_\rho}{dt} = \lambda_{\tau_\rho A_\beta} A_\beta + \lambda_{\tau_\rho} \tau_\rho (K_{\tau_\rho} - \tau_\rho) \\ \frac{d\tau_o}{dt} = \lambda_{\tau_o AS} \\ \frac{dN}{dt} = \lambda_{N\tau_o} \tau_o + \lambda_{N\tau_\rho} \tau_\rho + \lambda_N N (K_N - N) \\ \frac{dC}{dt} = \lambda_{CN} N + \lambda_C C (K_C - C) \end{cases} \quad (1)$$

where A_β represents amyloid pathology, τ_ρ represents amyloid-related tau pathology (p-tau), τ_o represents age-related and/or nonAD-related tau pathology, N represents neuronal dysfunction/loss, and C represents cognitive impairment. We define total tau pathology, τ, as the sum of τ_ρ and τ_o, namely, $\tau = \tau_\rho + \tau_o$. λ defines 9 rate constants. $\lambda_{A\beta}$, $\lambda_{\tau\rho}$, λ_N, and λ_C reflect the logistic growth rates of the various biomarker cascades. The remaining constants reflect linear growth rates of the biomarkers and determine the influence of various factors on the time-of-onset of the subsequent biomarker cascades. K defines the four biomarker carrying capacities $K_{A\beta}$, $K_{\tau\rho}$, K_N, and K_C, and A_0 defines the initial A_β level.

Data Sourcing and Selection

Individual longitudinal subject data for model personalization was sourced from ADNI, a multinational study that has provided new insights into the timeline of the evolution of AD biomarkers (6, 7). ADNI began in 2004 and comprises four sequential studies—ADNI-1, ADNI-GO, ADNI-2, and ADNI- 3—which followed subjects up to 15 years. Two overlapping cohort subsets of the ADNI dataset, as described below, were used to carry out the personalization and validation of the individual subject models. One included all 819 subjects in the ADNI-1 cohort, including those classified as having mild AD (N=192), late mild cognitive impairment (MCI, N=398), and normal cognition (N=229). The demographic distribution of subjects are displayed in the training subtable in Table 1. The second cohort, used for validation, included the subset of subjects in ADNI-1 with at least one future follow-up full biomarker dataset in ADNI-GO or ADNI-2 (N = 59) and is displayed in the testing subtable in Table 1.

Data Preparation

Serial scalar measures of cerebrospinal fluid (CSF) levels of amyloid-beta 42, phosphorylated tau 181, and total-tau were used as surrogates for amyloid, p-tau, and total tau pathology respectively. These measures were obtained through serial spinal taps on subjects over approximately two-year intervals. Of note, amyloid beta in the CSF goes down, and total and phosphorylated tau go up as the disease progresses. Hippocampal volume, based on MRI volumetrics at approximately one-year intervals, was used as a surrogate for neurodegeneration (8). It goes down as the disease progresses. Finally,

the thirteen-item Alzheimer Disease Assessment Scale (ADAS-13), measured at 6-month intervals, was used as a surrogate for cognitive decline. This measures function in several cognitive domains affected by AD, including memory, language, and praxis, and is the de facto primary outcome measure in AD clinical trials. It goes up as the disease progresses. Each biomarker measurement was scaled such that the middle 90% (7) of measurements fell into a fixed range between 0 and 1, which represent the theoretical minimum and maximum biomarker abnormality levels. This was done by setting X_{max} equal to the 95th percentile threshold of values and X_{min} equal to the 5th percentile threshold such that

$$X_{scaled} = \frac{X - X_{min}}{X_{max} - X_{min}}$$

where X represents the original value and X_{scaled} the scaled value. Because amyloid beta in the CSF and hippocampal volume go down as the disease progresses, the scaled values for both were subtracted from 1. In this way, all biomarker values would increase as the disease progresses.

Parameter Estimation

The system of differential equations was solved for each subject in the cohort using all available biomarker time points in the ADNI-1 dataset. The system of ODEs can be expressed as

$$\frac{d\boldsymbol{u}}{dt} = f(\boldsymbol{u}, \boldsymbol{p})$$

where $u = (A_\beta, \tau_\rho, \tau, N, C)^T$ represents the biomarker vector and p denotes the parameter vector on the right-hand side of the model. Then we can estimate the parameter p by solving the optimization problem given below:

$$\min_{\boldsymbol{p}} L(\boldsymbol{p}) := \sum_{i=1}^{n} \left\| \boldsymbol{u}(t_i; \boldsymbol{p}) - \tilde{\boldsymbol{u}}(t_i) \right\|^2 + \boldsymbol{\lambda} \left\| \boldsymbol{u}(100; \boldsymbol{p}) - \mathbf{1} \right\|^2 \qquad (2)$$

where $\tilde{u}$ (t_i) is the clinical data of a specific patient for given age t_i and u(t_i;p) is the biomarker solution of the AD model. This objective function is to minimize the L2 loss on given clinical patient data points and also incorporate the constraint of $u(100, p)=1$ by the penalty term. The highly non-convex nature of the optimization makes parameter estimation quite challenging. Therefore, we employed an optimization approach based on the "equation-by-equation" (EBE) algorithm (9). This approach involves fitting the amyloid biomarker first, followed by tau, neurodegeneration, and cognitive impairment. We used the fmin bfgs routine in Python, along with the EBE algorithm, and defined separate loss functions for each biomarker. For example, the optimization problem of the amyloid equation is defined as follows:

$$\min_{\lambda_{A_\beta}, K_{A_\beta}, A_o} \sum_{i=1}^{n} \left\| A_\beta\left(t_i; \lambda_{A_\beta}, K_{A_\beta}, A_o\right) - \widetilde{A_\beta}(t_i) \right\|^2 + \boldsymbol{\lambda} \left\| A_\beta\left(100; \lambda_{A_\beta}, K_{A_\beta}, A_o\right) - \mathbf{1} \right\|^2 \qquad (3)$$

where we incorporate the constraint of A_β (100)=1 by using the penalty term with λ=100 and during each iteration ODE solutions are determined by SciPy's ODE solver solve ivp. The parameter bounds were established for each biomarker through trial and error, and the parameter initialization was fixed for all biomarkers except for tau. The parameter estimation for tau was completed using the trust-region algorithm for constrained optimization, while the Broyden–Fletcher–Goldfarb–Shanno (BFGS) algorithm was used for all other biomarkers (10, 11). Therefore, for optimization, varying initial values for tau between its parameter bounds were used. After an initial optimization of parameters for each biomarker, multiple iterations of the optimization process were repeated on randomized initial parameter values obtained from a broader parameter space (between 80% and 120% of the initial optimization). The final personalized parameters were determined from the solutions to the ODE system with minimal loss. Fits were performed on all subjects. In the event a subject did not have any values for a particular biomarker, the missing parameters were substituted using the average parameter of the entire population of subjects as the initial value of the parameter.

Statistical Analysis

Summary statistics on demographics were calculated for the full ADNI-1 cohort, as well as the subset of subjects with at least one full biomarker follow-up dataset. Differences among diagnostic groups were tested using an ANOVA with posthoc testing, for continuous variables, and a Chi-square test for independence for categorical variables.

Summary statistics on the fourteen model parameters were calculated and stratified by diagnostic group. Subsequent statistical tests were performed directly on the derived model parameters, based on the assumption that the within-subject variance of the parameter estimates would be small with respect to the between-subject variance, as well as homoscedastic, that is, relatively equal across subjects (Figure S8).

Differences among the groups were tested for each of the parameters using an analysis of variance (ANOVA) with posthoc testing using a Bonferroni correction. The relationship of model parameters with risk factors, such as Apolipoprotein E4 carrier genetic status and years of prior education, was also evaluated, using a two-sample t-test and linear regression, respectively.

Personalized model fits were assessed by evaluating the error distribution across the entire training set. To evaluate the prediction error of the models, a subset of ADNI-1 subjects with at least one follow-up test datapoint in ADNIGO/ADNI- 2 for each of the biomarkers was

Table 1. Subject demographics of subjects

Training				
	CN	**MCI**	**AD**	**p-value**
# Subjects	229	402	188	-
Age (years)	75.9(5.0)	74.8(7.4)	75.2(7.5)	(0.043,0.323,0.448)
MMSE	29(0.99)	27(1.8)	23(2.0)	(<0.001,<0.001,<0.001)
Testing				
	CN	**MCI**	**p-value**	
# Subjects	32	27	-	
Age (years)	74.8(5.7)	73.0(5.8)	0.249	
MMSE	29.1(1.1)	27.4(1.8)	<0.001	
Gender	16 F, 16M	8 F, 19M	0.187	
Education (years)	16.2(3.0)	16.7(2.7)	0.524	

Top: Subject demographics given as their mean (SD) in full cohort of 819 training subjects from ADNI-1. Group designations are those at entry into ADNI-1. MMSE-Mini Mental State Examination; CN-Cognitively Normal; MCI-Mild Cognitive Impairment; AD- Alzheimer's Disease; NS-not significant; Age and Education are in units of years. All values are mean (SD). Pairwise t-tests were only performed if the omnibus p-value was significant ($p < 0.05$, Bonferroni corrected). P-values are displayed pair-wise as (CN-MCI, CN-AD, MCI-AD). Bottom: Subject demographics on 59 training subjects from the ADNI-1 cohort with at least one complete ADNI-GO/2 dataset for testing. Data is taken from the date of entry to the ADNI-1 study. MMSE- Mini Mental State Examination; CN-Cognitively Normal; MCI-Mild Cognitive Impairment; AD-Alzheimer's Disease; NS-not significant; Age and Education are in units of years.

used. Subjects were trained on all available ADNI-1 biomarker data and tested on the first available time-point in follow-up. All data preparation steps performed on the training data were performed on the test set, including scaling to the training data. Model performance was assessed using root mean squared error (RMSE) and intraclass correlation (ICC) (one-way random effects) between the predicted and actual biomarker values for the four biomarker test points in each subject. Model bias was assessed using Bland-Altman plots. For a performance benchmark, empirical linear fits on single biomarker training data were performed and prediction error between the explanatory and empirical models was compared. Prediction error as a function of the number of available complete biomarker training datasets was also evaluated using both linear and exponential fits.

To assess whether model parameters would yield distinct endophenotypes, we performed a cluster analysis of the parameters across the entire population of 819 subjects using K-nearest-neighbors (KNN) (n=3) after dimension reduction with principal components analysis. Cluster number n=3 was chosen to match the number of clinical phenotypes in the sample (CN, MCI, and AD). Silhouette and Rand's scores were used to evaluate the quality of the clusters created and the degree to which they matched the known clinical phenotypes established at study's outset. Biomarker characteristics were then compared across the clusters using an ANOVA with posthoc analysis.

Results

Demographics

Summary statistics are given for the entire ADNI-1 cohort at the beginning of the study (Table 1, top). As expected, there was a significant difference with respect to MMSE distribution among diagnostic groups. In addition, there was a bias toward the male gender for the MCI group, and there were fewer years of education in the AD group compared to the other two groups. There were no significant differences among groups with respect to age. Summary statistics are also given for the subset of subjects from ADNI-1 with at least one full test set from ADNI-GO/ADNI-2 (Table 1, bottom). There was a significant difference in MMSE among the two diagnostic groups represented, CN and MCI, as expected, but no significance for age, gender, or education.

Parameter Evaluation

Mean values of the fourteen model parameters are displayed in Table 2, separated by parameter type and stratified by initial diagnosis in ADNI-1. Seven of fourteen parameters showed an overall significant effect on the diagnostic group ($p < 0.05$) by ANOVA, including all four neurodegeneration parameters, and two of the three cognitive decline parameters. Figure S1 displays box and whisker plots stratified by diagnostic group. Table S1 shows the relationship between genetic and education status with the model parameters. At least one parameter from each of the four biomarker equations showed a significant relationship with APOE4 carrier status. Only one parameter, $\lambda\tau_{\varphi}$, showed a significant relationship with years of education.

Table 2. Model parameter summary table

Equation 1 Biomarker	Parameter	CN	MCI	AD	Pairwise p-val
A_β	KA_β	1.4(0.96)	1.2(0.81)	1.2(0.71)	(0.033, 0.012, 0.477)
	λA_β	0.18(0.094)	0.2(0.11)	0.21(0.11)	(0.002, 0.004, 0.635)
	A_0	0.021(0.03)	0.03(0.04)	0.03(0.04)	(0.041, 0.023, 0.523)
τ	$K\tau_\rho$	1.03(1.81)	0.91(1.9)	0.75(1.73)	(0.439, 0.110, 0.311)
	$\lambda\tau_\rho A_\beta$	9E-3(0.015)	9E-3(0.012)	8E-3(0.011)	(0.815, 0.337, 0.342)
	$\lambda\tau_\rho$	0.48(0.24)	0.51(0.23)	0.54(0.22)	(0.093, 0.0072, 0.155)
	$\lambda\tau_o AS$	5E-3(1E-3)	5E-3(2E-3)	6E-3(2E-3)	(<0.001, <0.001, 0.0028)
N	K_N	1.19(0.5)	1.07(0.3)	1.02(0.11)	(<0.001, <0.001, 0.012)
	$\lambda N\tau_\rho$	0.013(0.04)	5E-3(0.02)	1E-3(6E-3)	(<0.001, <0.001, 0.0029)
	λ_N	0.20(0.16)	0.25(0.15)	0.31(0.15)	(<0.001, <0.001, <0.001)
	$\lambda N\tau_o$	3E-3(7E-3)	1E-3(5E-3)	1E-3(5E-3)	(0.0053, <0.001, 0.145)
C	K_C	1.82(2.6)	1.1(0.7)	0.96(0.14)	(<0.001,< 0.001,< 0.001)
	λ_C	0.21(0.17)	0.27(0.17)	0.37(0.15)	(<0.001,< 0.001,< 0.001)
	λ_{CN}	0.025(0.03)	0.02(0.03)	0.02(0.03)	(0.93, 0.0043, 0.0014)

Model parameter summary statistics - Mean (SD); CN-Cognitively Normal; MCI-Mild Cognitive Impairment; AD- Alzheimer's Disease. Pairwise tests were only performed if the omnibus p-value was significant ($p < 0.05$, Bonferroni corrected). P-values are displayed pairwise as (CN-MCI, CN-AD, MCI-AD).

Figure 1. The Alzheimer disease biomarker cascade model

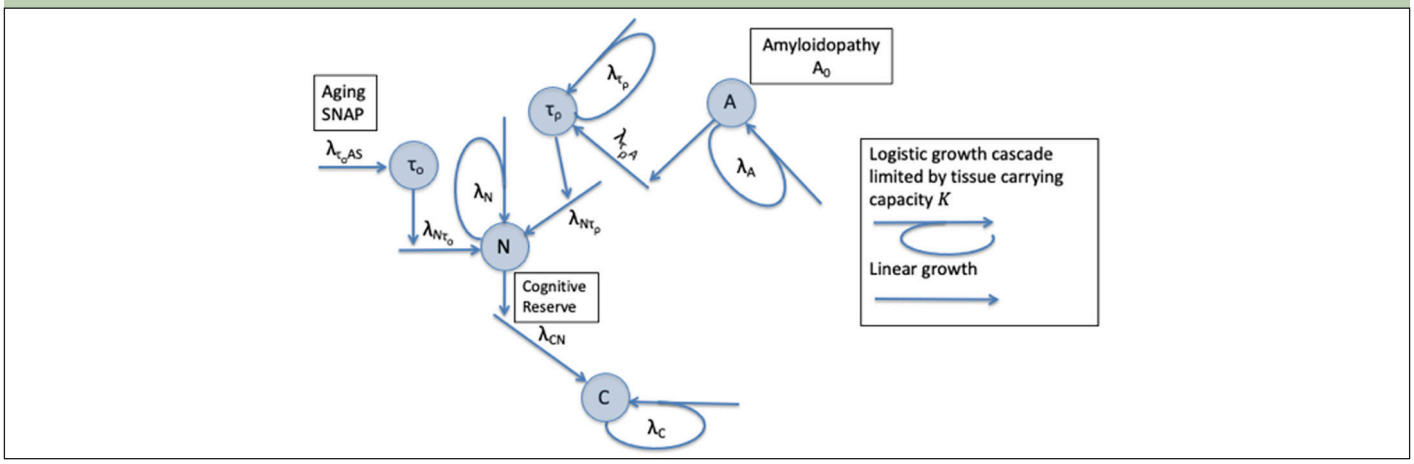

Diagram depicting dynamic causal modeling implementation of the biomarker cascade model in Alzheimer's disease (Adapted from (3)). Blue circles represent biomarker quantities. A_β represents amyloid beta pathology. Its initial value A_0 determines when during the lifespan the amyloid cascade begins. τ_ρ represents phosphor-tau (p-tau) or amyloid-related tau pathology. τ_o represents age-related and/or suspected non- Alzheimer pathology (SNAP)-related tauopathy. N represents neuronal dysfunction/loss. C represents cognitive impairment. λ values are growth rate constants.

Model Performance

Examples of personalized biomarker trajectories for nine different subjects from the ADNI-1 cohort are shown in Figure 2. The distribution of model training error in the ADNI-1 data set across all subjects is shown in Figure S2. Over all biomarkers, within-subject variance was small relative to the between-subject variance. We chose the root mean squared error (RMSE) as a measure of performance for each subject because it is in the same scale as the scaled biomarker variables between 0 and 1. We also report mean absolute percentage error (MAPE) as a scale free measure in the Supplementary Material (Figures S3 and S6).

Across all subjects, the mean RMSE for training error was 0.09 (SD 0.081), with 745 of 819 (91%) subjects showing RMSE < 0.2. To evaluate the prediction error of the model, we used a subset of 59 subjects in ADNI-1, all of whom had at least one complete biomarker test set in the follow-up studies ADNI-2 or ADNI-GO. Predicted biomarker trajectories along with plots of training and test points for this subset are shown in Figure S4. The mean time between the last ADNI-1 training timepoint and the first ADNI2/GO test timepoint was 427 (SD 151.4) days. Prediction error distribution is shown for the ODE model in Figure S5. The mean RSME for the ODE model was 0.15 (SD 0.117). Approximately 80% (47 of 59) of subjects had an RMSE less than 0.2. For the reference linear model RMSE was 0.16 (SD 0.121). There

Figure 2. Biomarker trajectories across diagnostic groups

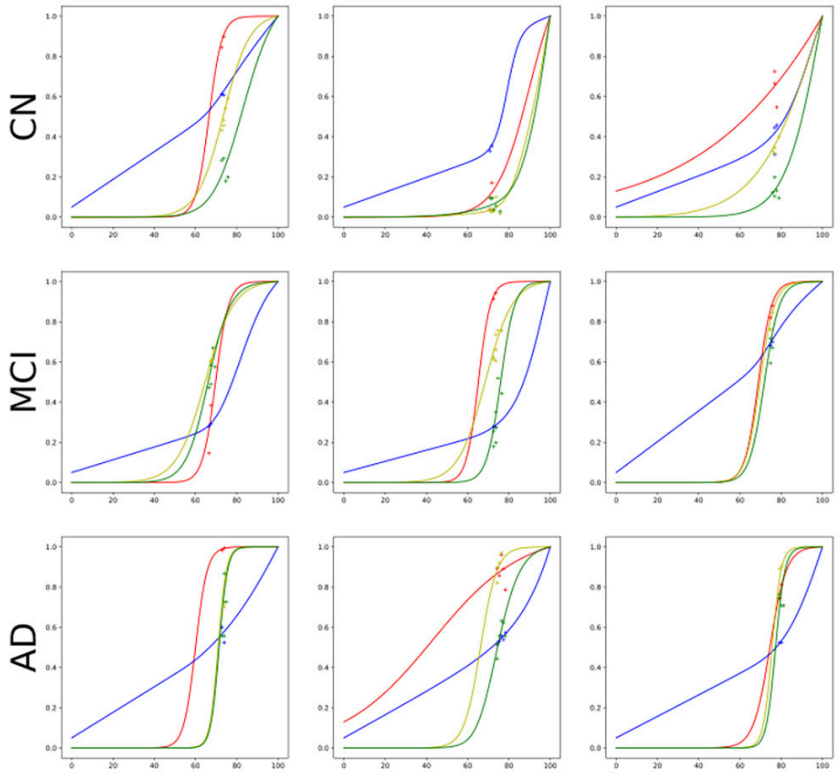

Example biomarker trajectories for nine different subjects from ADNI-1 cohort. The rows represent ADNI-1 entry diagnostic groups (CN – cognitively normal, MCI – mild cognitive impairment, AD – mild Alzheimer's disease. The color lines denote the individual biomarker trajectory fits over the lifespan (Red – amyloid, Blue - total tau, Yellow – neurodegeneration, Green – cognitive decline). Crosses in the graph represent the training data from ADNI-1 for the model in each case, whereas solid dots represent the testing data in ADNI-2/GO if it exists. Note the variability of biomarker trajectories across traditional clinical phenotypes. All AD subjects, for example, show high total tau levels early in life; however the timing of amyloid and neurodegeneration is different. The middle AD subject in the figure is driven by early life amyloid deposition and neurodegeneration; whereas the first shows mid-life amyloid and the last late life amyloid deposition, both with late neurodegeneration. Similarly, MCI subjects show variable tau levels early in life. The first two MCI subjects show low tau levels early in life with acceleration after the appearance of amyloid in late-middle age; whereas the third MCI subject shows high total tau levels early in life, age in onset of cognitive impairment in 70's. These results reaffirm the biological heterogeneity within diagnostic labels and support the idea of multiple disease drivers contributing to cognitive phenotype.

was no statistically significant difference between the prediction error between the ODE and linear models on a two-tailed paired student's t-test ($p = 0.126$). The prediction error for the ADNI-2/GO test timepoint as a function of the number of complete datasets in ADNI-1 is shown in Figure S7. Prediction error (RMSE) dropped to below 0.2 with one or more complete training datasets per subject. For these subjects with at least one complete biomarker training set (N=53), a scatterplot of predicted vs. actual values of the ODE model is shown in Figure 3 for all four biomarkers along with their ICC values. The overall ICC value for all four biomarkers combined was 0.90, compared to 0.88 for the comparison linear model (Figure S10). Of the four biomarkers, neurodegeneration, as determined by hippocampal volume, showed the highest correlation between predicted and actual values with an ICC value of 0.95. No significant under- or over-estimation prediction bias was demonstrated for any of the four biomarkers. Bland-Altman plots are given in Figure S8.

Cluster Analysis

KNN cluster analysis (N=3) of model parameters is shown graphically in Figure S9 using the first two principal components of the fourteen model parameters. Three overlapping clusters emerged (Silhouette score = 0.43). The Silhouette score, which ranges between -1 and +1, suggested that clustering was only fair for the three clusters. Moreover, there was no significant similarity to the three diagnostic groups when the diagnostic group label was taken as ground truth (Rand score = 0.50). The Rand score of 0.5 was indicative of random cluster assignment with respect to the three diagnostic group labels.

However, significant differences were present with respect to biomarkers and cognitive indices among at least two of the clusters suggesting the existence of at least two distinct endophenotypic groups (Table S2). Cluster number 2 showed a significantly higher proportion of cognitively normal phenotypes, higher hippocampal volumes, MMSE scores, and CSF a-beta levels, and significantly lower ADAS13 and CDR-SOB scores, and CSF tau and p-tau protein levels. In addition,

Figure 3. Scatterplots of predicted vs. actual biomarker values

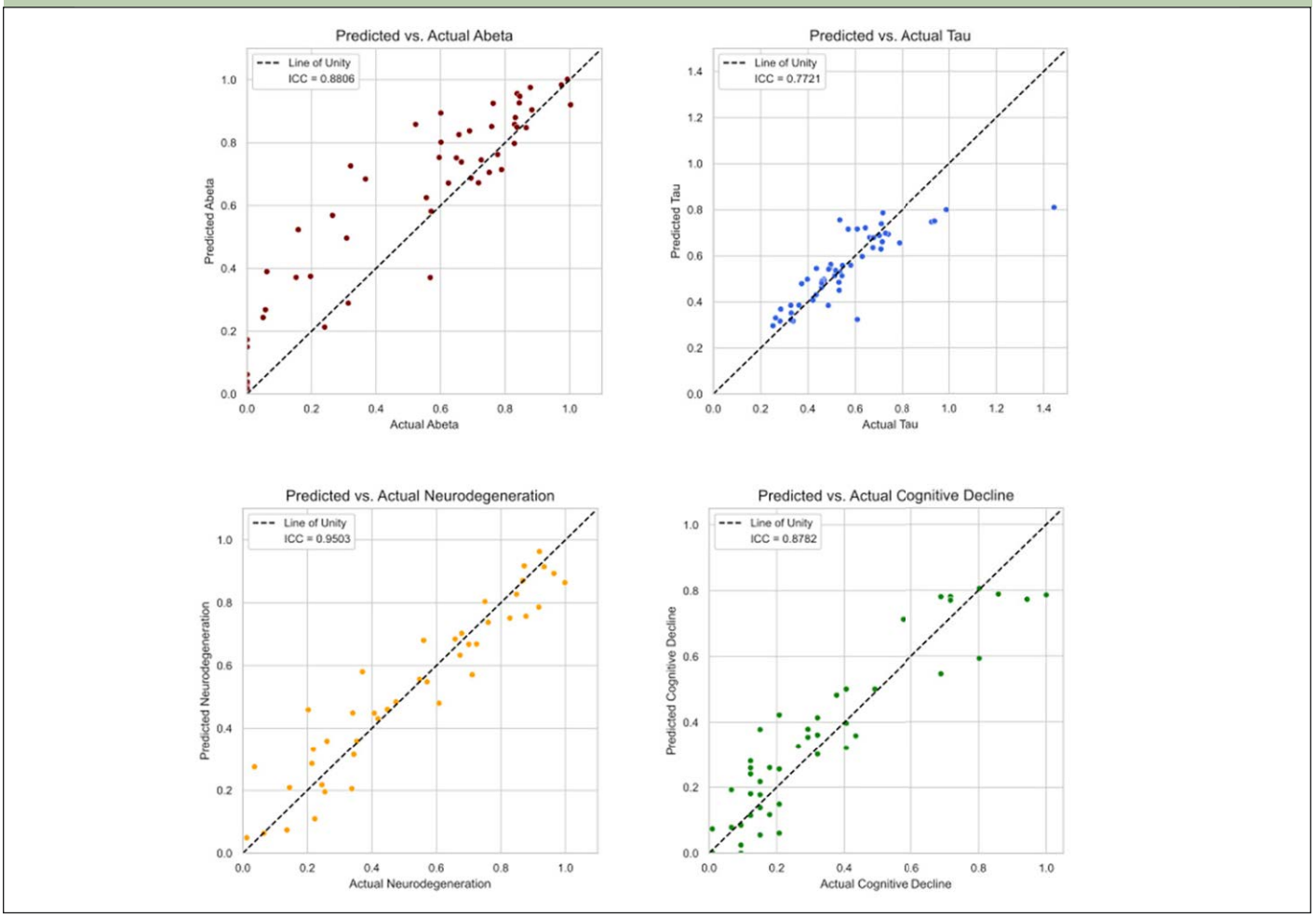

Scatterplots of predicted vs. actual biomarker value of cohort of subjects with at least one complete set of biomarkers in ADNI-1 and at least one complete set of biomarkers in ADNI-2/GO (n=53). ADNI-1 datapoints were used to generate the predicted biomarker for ADNI-2/GO using the ODE model, which was then compared with the actual value. ICC-Intraclass Correlation Coefficient.

over time, fewer CN and MCI subjects converted to AD in this group, 12% compared to 30% and 34% in clusters 1 and 0, respectively. Moreover, ADAS13 and CDR-SOB scores increased the least in cluster 2, less than 20% of that of the other two clusters. Cluster 2 demonstrated a higher weighting of principal component number 1. The weightings of the principal components are given in the legend to Figure S9. In general, component 1 negatively weighted downstream parameters related to the rate of neurodegeneration, λ_N, the rate of cognitive decline, λ_C, and the rate of phosphorylated tau accumulation, $\lambda\tau_\rho$, while positively weighting latency parameters related to the effect of τ_o and τ_ρ on neurodegeneration, $\lambda_{N\tau o}$ and $\lambda_{N\tau\rho}$, respectively.

Discussion

In this study, we analyzed the feasibility of personalizing a time-dependent causal model of AD progression with longitudinal biomarker data from subjects across the AD cognitive spectrum. As a proof-of-concept, we chose a widely- referenced hypothetical model of AD, based on the amyloid cascade hypothesis, which we had previously implemented mathematically as a mechanistic model. This integrative model, the ADBC model, consists of a sparse system of differential equations involving four measurable biomarkers based on CSF, imaging, and cognitive data. Personalization of the ADBC model in over 800 subjects from ADNI with serial biomarker data yielded fourteen personalized parameters reflecting physiologically meaningful characteristics including growth rates, latency values, and carrying capacities of the various biomarkers, many of which demonstrated significant differences across clinical diagnostic groups. Moreover, several of the parameters showed significant relationships with factors known to modify AD risk, namely APOE carrier status, and to a lesser extent, education status, consistent with the idea that genetics has a greater effect compared to education on the biology of the disease (12).

The model fits to training data across the entire cohort had an RMSE of 0.09 (SD 0.081) on a variable scale between zero and one, and were robust, with over 90% of subjects showing an RMSE of < 0.2. Similarly, in a subset

of subjects with data on all four biomarkers in at least one test set, performance was high on the test sets, with a mean RMSE of 0.15 (SD 0.117), with 80% of subjects demonstrating an RMSE < 0.2 in the estimation of future biomarker points. These results support the feasibility of personalizing mechanistic models based on individual biomarker trajectories.

The performance of the mechanistic ODE model was not a significant improvement over simple linear models of single biomarker trajectories. This may be due to the sparse nature of the mechanistic model and does not diminish the importance of establishing the feasibility of the personalized causal modeling approach. Empiric predictive models may often outperform causal/explanatory models but do not have the same advantages in terms of discovering underlying disease drivers and predicting therapeutic responses. As our understanding of AD increases and further complexity becomes incorporated, the integrative, mechanistic nature of a more refined ADBC model might have less bias, and therefore ultimately better performance, compared to simpler empiric approaches.

The performance of the model improved when there was at least one complete biomarker training time point, with diminishing returns in subjects with more time points available. After two complete training datasets, prediction error appeared to level off as revealed by the better fit of an exponential, as opposed to linear, function to the data in Figure S7. This may have to do with the fact that the mechanistic model imposed fixed initial conditions and constraints creating additional anchor points for establishing biomarker trajectory. For example, one constraint specified in the ADBC model was that biomarkers levels reached their maximum by age 100. This was imposed in the ADBC model to operationalize the description of the biomarker cascade hypothesis in which biomarker slopes generally accelerate in older age (2). The requirement for only one-time point of biomarker training data would make clinical applications of the model more feasible in patients for whom only one-time point's worth of biomarker data may be available before decisions must be made regarding clinical trial selection or therapy.

Cluster analysis of parameters revealed up to three clusters, without significant correspondence to clinical labels, as evidenced by a Rand score near 0.5. Among the three clusters, one distinct biomarker endophenotype emerged. Cluster 2 appears to represent a cognitively healthier endophenotype, with more favorable atrophy and CSF biomarker profile, compared to the other two clusters, and less cognitive decline over time (Table S2). This endophenotype was represented by a higher weighting of principal component 1, representing in the model lower rates of neurodegeneration, cognitive decline, and tau accumulation, and a longer latency between the onset of tau pathology and neurodegeneration (Figure S9). This separation of endophenotype, based on model parameters, suggests that modeling of biomarkers based on a mechanistic analysis of biomarker trajectories may be useful for reclassifying subjects on the AD spectrum. This is particularly important for subjects that fall into the heterogenous MCI clinical diagnostic category, where subjects may progress to AD, remain stable, or even revert to a cognitively normal state (13). Previous evidence using cluster analysis on longitudinal biomarker data in MCI subjects also suggests two distinct clusters, consisting of rapid and slow decliners (14). Figure 2 shows example biomarker trajectories for three subjects in each of the ADNI-1 entry diagnostic groups. Note how biomarker profiles are heterogenous both within and between groups defined by clinical diagnosis alone.

Previous work in mathematical modeling of AD progression, with a focus on mechanistic models, has recently been the subject of a scoping review (15). Of the previous 17 mechanistic mathematical models described, only four were validated against patient data with none of those four studying personalized models and underlying disease trajectories in individual patients (16-19). The majority of work used ordinary or partial differential equations and modeled AD at the cellular scale and on a short time scale, such as minutes to hours. Few considered more than two factors, such as amyloid-beta and tau, as factors in the model (4, 16-18, 20-24). Though not yet validated with patient data, the ADBC model (4) was the only mechanistic model reviewed that included clinically available biomarkers, including measures of cognition and neurodegeneration, and modeled over the lifespan. The current work, using available serial biomarker data in over 800 subjects across the cognitive spectrum, helps validate the ADBC model as a useful starting point for mechanistic modeling of clinically available AD biomarkers. The resulting model parameters and biomarker trajectories may yield more nuanced information in individual patients compared to single or serial biomarker levels.

This work has a number of limitations. Attempting to predict long-term disease trajectory over decades from short- term data, usually within one decade, is difficult and sensitive to noise in the data, particularly for estimating the rate constants of the biomarkers which require accurate estimation of slope. Having constraints that anchored the biomarkers at time = 0 and time = 100 (years) helped reduce this sensitivity. Nevertheless, the extent to which this assumption is incorrect will bias the model, and future versions of the model may have to be restricted to one or two decades. Identifiability analysis (25) may be of value in determining how well the ADBC model personalized parameters can be determined by the sparse individual longitudinal data in ADNI. To improve identifiability, sensitivity analysis may aid in creating a more parsimonious model by setting low variance parameters to a constant. Previous groups have attempted to address recovering long-term disease trends

from short-term data using a semiparametric model to estimate the temporal ordering of biomarkers and long-term growth curves (26, 27). However, these approaches have used empirical functions to fit the data, rather than a mechanistic model of disease, which is the focus of our current approach. Other groups have used a disease progression score to replace time as the independent variable to incorporate cross-sectional data in formulating a population-based disease progression model. This was accomplished by shifting and scaling individual subject data, based on different ages of onset and progression rates of disease (28, 29). Because the aim of this research is to create personalized models of disease, such work would only apply here to using population-derived parameters as initial values prior to personalization. Another limitation related to short-term data is the short follow-up duration in the test data derived from the follow-on studies ADNI-GO and ADNI-2. The mean follow-up time was 1-2 years, which could be considered short in terms of the lifespan, nevertheless is a clinically relevant follow-up interval, often used in Alzheimer's disease clinical trials (30). Lastly, the data used to parameterize the ADBC model was obtained from a single data source, ADNI, which represents a convenience sample over-represented by an educated, predominantly Caucasian population (https://www.adni-info.org/). Thus, the generalization of the parameters calculated in this model to a community setting with subjects across the cognitive spectrum will be limited.

In summary, we have shown the feasibility of personalizing a causal model of AD progression, the ADBC model, an integrative biomarker model based on the amyloid cascade hypothesis. Personalization of this model with longitudinal biomarker data from over 800 subjects across the AD cognitive spectrum yielded fourteen personalized parameters reflecting physiologically meaningful characteristics. Model fits were robust and performance on unseen test data was moderate to high, with 80% of subjects demonstrating prediction error within 20% with only a single complete biomarker training set, suggesting that this model may be useful for cases when longitudinal data is not available, for example, in clinical trial or patient care settings. Cluster analysis of parameters revealed distinct endophenotypic clusters, suggesting that the model may be useful for reclassifying subjects on the AD spectrum. Future studies are warranted to refine the current personalized model as a tool for discovering individual disease drivers, predicting natural history, and ultimately, simulating the effects of therapeutic interventions.

Funding: JRP was supported in part by the National Science Foundation (NSF) [DMS-2052676]. WH was supported in part by NSF [DMS-2052685] and NIH [1R35GM146894]. Data collection and sharing for this project was funded by the Alzheimer's Disease Neuroimaging Initiative (ADNI) (National Institutes of Health Grant U01 AG024904) and DOD ADNI (Department of Defense award number W81XWH-12-2-0012). ADNI is funded by the National Institute on Aging, the National Institute of Biomedical Imaging and Bioengineering, and through generous contributions from the following: AbbVie, Alzheimer's Association; Alzheimer's Drug Discovery Foundation; Araclon Biotech; BioClinica, Inc.; Biogen; Bristol-Myers Squibb Company; CereSpir, Inc.; Cogstate; Eisai Inc.; Elan Pharmaceuticals, Inc.; Eli Lilly and Company; EuroImmun; F. Hoffmann-La Roche Ltd and its affiliated company Genentech, Inc.; Fujirebio; GE Healthcare; IXICO Ltd.;Janssen Alzheimer Immunotherapy Research & Development, LLC.; Johnson & Johnson Pharmaceutical Research & Development LLC.; Lumosity; Lundbeck; Merck & Co., Inc.; Meso Scale Diagnostics, LLC.; NeuroRx Research; Neurotrack Technologies; Novartis Pharmaceuticals Corporation; Pfizer Inc.; Piramal Imaging; Servier; Takeda Pharmaceutical Company; and Transition Therapeutics. The Canadian Institutes of Health Research is providing funds to support ADNI clinical sites in Canada. Private sector contributions are facilitated by the Foundation for the National Institutes of Health (www.fnih.org). The grantee organization is the Northern California Institute for Research and Education, and the study is coordinated by the Alzheimer's Therapeutic Research Institute at the University of Southern California. ADNI data are disseminated by the Laboratory for Neuro Imaging at the University of Southern California. PMD was supported by a grant from ADNI.

Acknowledgements: We would like to express our sincere gratitude to Rohit Raguram for his valuable contribution in writing the initial code for this project, and for financial support during the initial stages of this project from Patricia S. Beach, in memory of her husband, James Robert Beach.

** Data used in preparation of this article were obtained from the Alzheimer's Disease Neuroimaging Initiative (ADNI) database (adni.loni.usc.edu). As such, the investigators within the ADNI contributed to the design and implementation of ADNI and/or provided data but did not participate in analysis or writing of this report. A complete listing of ADNI investigators can be found at: http://adni.loni.usc.edu/wp-content/uploads/how_to_apply/ADNI_Acknowledgement_List.pdf

Ethical standards: ADNI was approved by IRBs of all participating sites and all subjects gave written informed consent for data collection and sharing. This report is solely an analysis of deidentified data and hence is exempt under human subjects research.

Conflict of interest: JRP has served on medical advisory boards for cortechs.ai, Biogen and icometrix. PMD has received grants, advisory/board fees and/or stock from several health and technology companies. PMD is a co- inventor on several patents for the diagnosis or treatment of dementias. No competing interest is declared for other authors.

Data availability: Access to the ADNI dataset is publicly available via http://adni.loni.usc.edu.

References

1. Voit EO. Systems Biology in Medicine and Drug Development. In: Science G, editor. A First Course in Systems Biology: Taylor & Francis Group, LLC; 2013. p. 347-72.
2. Jack CR, Jr., Holtzman DM. Biomarker modeling of Alzheimer's disease. Neuron. 2013;80(6):1347-58.
3. Jack CR, Jr., Knopman DS, Jagust WJ, Petersen RC, Weiner MW, Aisen PS, et al. Tracking pathophysiological processes in Alzheimer's disease: an updated hypothetical model of dynamic biomarkers. Lancet neurology. 2013;12(2):207-16.
4. Petrella JR, Hao W, Rao A, Doraiswamy PM. Computational Causal Modeling of the Dynamic Biomarker Cascade in Alzheimer's Disease. Comput Math Methods Med. 2019;2019:6216530.
5. Hao W, Lenhart S, Petrella JR. Optimal anti-amyloid-beta therapy for Alzheimer's disease via a personalized mathematical model. PLoS Comput Biol. 2022;18(9):e1010481.
6. Weiner MW, Veitch DP, Aisen PS, Beckett LA, Cairns NJ, Cedarbaum J, et al. Impact of the Alzheimer's Disease Neuroimaging Initiative, 2004 to 2014. Alzheimers Dement. 2015;11(7):865-84.
7. Weiner MW, Veitch DP, Aisen PS, Beckett LA, Cairns NJ, Green RC, et al. The Alzheimer's Disease Neuroimaging Initiative 3: Continued innovation for clinical trial improvement. Alzheimers Dement. 2017;13(5):561-71.
8. Tanpitukpongse TP, Mazurowski MA, Ikhena J, Petrella JR, Alzheimer's Disease Neuroimaging I. Predictive Utility of Marketed Volumetric Software Tools in Subjects at Risk for Alzheimer Disease: Do Regions Outside the Hippocampus Matter? AJNR Am J Neuroradiol. 2017;38(3):546-52.
9. Hao WR, Harlim J. An Equation-by-Equation Method for Solving the Multidimensional Moment Constrained Maximum Entropy Problem. Comm App Math Com Sc. 2018;13(2):189-214.
10. Fletcher R. Practical Methods of Optimization. New York: John Wiley & Sons; 1987.
11. Sorensen DC. Newton's Method with a Model Trust Region Modification. SIAM Journal on Numerical Analysis. 1982;19(2):409-26.
12. Ma H, Zhou T, Li X, Maraganore D, Heianza Y, Qi L. Early-life educational attainment, APOE epsilon4 alleles, and incident dementia risk in late life. Geroscience. 2022;44(3):1479-88.

13. Petersen RC. Mild Cognitive Impairment Criteria in Alzheimer's Disease Neuroimaging Initiative: Meeting Biological Expectations. Neurology. 2021;97(12):597-9.
14. Gamberger D, Lavrac N, Srivatsa S, Tanzi RE, Doraiswamy PM. Identification of clusters of rapid and slow decliners among subjects at risk for Alzheimer's disease. Sci Rep. 2017;7(1):6763.
15. Moravveji S, Doyon N, Mashreghi J, Duchesne S. A Scoping Review of Mathematical Models Covering Alzheimer's Disease Progression. bioRxiv. 2022:1-11.
16. Hoore M, Khailaie S, Montaseri G, Mitra T, Meyer-Hermann M. Mathematical Model Shows How Sleep May Affect Amyloid-beta Fibrillization. Biophys J. 2020;119(4):862-72.
17. Lindstrom MR, Chavez MB, Gross-Sable EA, Hayden EY, Teplow DB. From reaction kinetics to dementia: A simple dimer model of Alzheimer's disease etiology. PLoS Comput Biol. 2021;17(7):e1009114.
18. Liu H, Wei C, He H, Liu X. Evaluating Alzheimer's Disease Progression by Modeling Crosstalk Network Disruption. Front Neurosci. 2015;9:523.
19. Pallitto MM, Murphy RM. A mathematical model of the kinetics of beta-amyloid fibril growth from the denatured state. Biophys J. 2001;81(3):1805-22.
20. Hao W, Friedman A. Mathematical model on Alzheimer's disease. BMC Syst Biol. 2016;10(1):108.
21. Helal M, Hingant E, Pujo-Menjouet L, Webb GF. Alzheimer's disease: analysis of a mathematical model incorporating the role of prions. J Math Biol. 2014;69(5):1207-35.
22. Helal M, Igel-Egalon A, Lakmeche A, Mazzocco P, Perrillat-Mercerot A, Pujo-Menjouet L, et al. Stability analysis of a steady state of a model describing Alzheimer's disease and interactions with prion proteins. J Math Biol. 2019;78(1-2):57-81.
23. Kuznetsov IA, Kuznetsov AV. How the formation of amyloid plaques and neurofibrillary tangles may be related: a mathematical modelling study. Proc Math Phys Eng Sci. 2018;474(2210):20170777.
24. Kuznetsov IA, Kuznetsov AV. Simulating the effect of formation of amyloid plaques on aggregation of tau protein. Proc Math Phys Eng Sci. 2018;474(2220):20180511.
25. Gabor A, Villaverde AF, Banga JR. Parameter identifiability analysis and visualization in large-scale kinetic models of biosystems. BMC Syst Biol. 2017;11(1):54.
26. Donohue MC, Jacqmin-Gadda H, Le Goff M, Thomas RG, Raman R, Gamst AC, et al. Estimating long-term multivariate progression from short-term data. Alzheimers Dement. 2014;10(5 Suppl):S400-10.
27. Fonteijn HM, Modat M, Clarkson MJ, Barnes J, Lehmann M, Hobbs NZ, et al. An event-based model for disease progression and its application in familial Alzheimer's disease and Huntington's disease. Neuroimage. 2012;60(3):1880-9.
28. Iturria-Medina Y, Carbonell FM, Sotero RC, Chouinard-Decorte F, Evans AC, Alzheimer's Disease Neuroimaging I. Multifactorial causal model of brain (dis)organization and therapeutic intervention: Application to Alzheimer's disease. Neuroimage. 2017;152:60-77.
29. Jedynak BM, Lang A, Liu B, Katz E, Zhang Y, Wyman BT, et al. A computational neurodegenerative disease progression score: method and results with the Alzheimer's disease Neuroimaging Initiative cohort. Neuroimage. 2012;63(3):1478-86.
30. Ritchie M, Gillen DL, Grill JD. Recruitment across two decades of NIH-funded Alzheimer's disease clinical trials. Alzheimers Res Ther. 2023;15(1):28.

How to cite this article: J.R. Petrella, J. Jiang, K. Sreeram, et al. Personalized Computational Causal Modeling of the Alzheimer Disease Biomarker Cascade. J Prev Alz Dis 2024;2(11):435-444; http://dx.doi.org/10.14283/jpad.2023.134